Progress In Electromagnetics Research M, Vol. 12, 67–79, 2010

EFFECTIVE PLASMA FREQUENCY FOR TWO-DIMENSIONAL METALLIC PHOTONIC CRYSTALS

K. L. Low, M. Z. Mat Jafri, and S. A. Khan

Universiti Sains Malaysia
Penang, Malaysia

Abstract—Generalized band structure equation for photonic crystals which containing dielectric rods in metals medium was derived by using the plane wave expansion method. From the band structure, we can study band gap of photonic crystals in both E and H polarizations. Since metals are frequency-dependant materials, modification needs to be done on the plane wave expansion equation to calculate the metallic photonic crystals containing dielectric constant rods. To ease the calculation, simple Drude model for metals are used. In this model, the equation is without damping constant. We have plotted the band structure for photonic crystals in metals medium. Then, we studied the effective plasma frequency of the structure from the band graph in E polarization mode (TM). We found that effective plasma frequency can be tailored as we want. Detailed results are presented with different sizes of radius. Comparison is made for different background materials.

1. INTRODUCTION

The photonic crystals have been extensively developed for the past 20 years. It is used as antenna [1–4], microstrip [1], solar cells [2, 3], fiber optic [4, 5], waveguide [6], etc. The materials that are being used for photonic crystals range from normal dielectric material to superconductor. But, we would like to discuss the properties of photonic crystals in metals medium in this article. Metals are frequency dependant material. We have used the Drude model to describe the dielectric constant of metal as follows:

$$\varepsilon(\omega) = 1 - \frac{\omega_p^2}{\omega\left(\omega - i\gamma\right)} \tag{1}$$

Corresponding author: K. L. Low (bennywt@gmail.com).

where ω_p is the plasma frequency, and γ is damping constant. Damping constant is neglected because it is small compared to plasma frequency [7]. So, we obtained a simple Drude model which the imaginary part of Equation (1) is neglected.

$$\varepsilon(\omega) = 1 - \frac{\omega_p^2}{\omega^2} \tag{2}$$

Plasma frequency is a basic constant that characterizes a metal. It cannot be changed. From the ordinary metallic band graph, it is the frequency at the minimum of the lowest band in a band energy graph. But, if the fundamental plasma frequency of metals can be modified as desired, it can be used widely in many areas. It is known that the plasma frequency is in the range of $\sim 10^{15}$ Hz which is in ultraviolet region. Pendry et al. [8] showed that plasma frequency of a periodic structure built of metallic thin wires can be depressed into GHz region or far infrared region. The results are promising. Brand et al. [9] reviewed previous studies and discussed the effective plasma frequency. Here we would like to study the effective plasma frequency of photonic crystals with dielectric rods in metals medium. We can arrive at the value by plotting the band energy graph of the structure. This calculation is very important but is left out by several authors. So, we have to derive the equation and plot the band energy graph. The effective plasma frequency is the minimum value at the lowest band. There are many methods proposed to find the band energy graph [1, 10–16]. Each method has its own limitation especially when frequency dependant material is considered. But, it has been reported that plane wave expansion method is capable to solve the metallic-vacuum photonic crystals in E polarization [17]. However, it is only limited in vacuum rods. Therefore, in this article we extended the study into metallic and dielectric rods by using the plane wave expansion method. Xu et al. [18] studied effective plasma frequency of 1-dimension metallic-dielectric photonic crystals but we studied plasma frequency in 2-dimension with different dielectric rods, and we would also theoretically study the effect of different cylinder materials that were inserted into the metallic structure.

2. METHOD

2.1. Basic

The 2D structure is shown in Figure 1. We assumed that the periodic structure is along z axis. We made assumption that the structure was infinitely long, parallel and symmetry structure. We implied that the structure thickness was infinite.

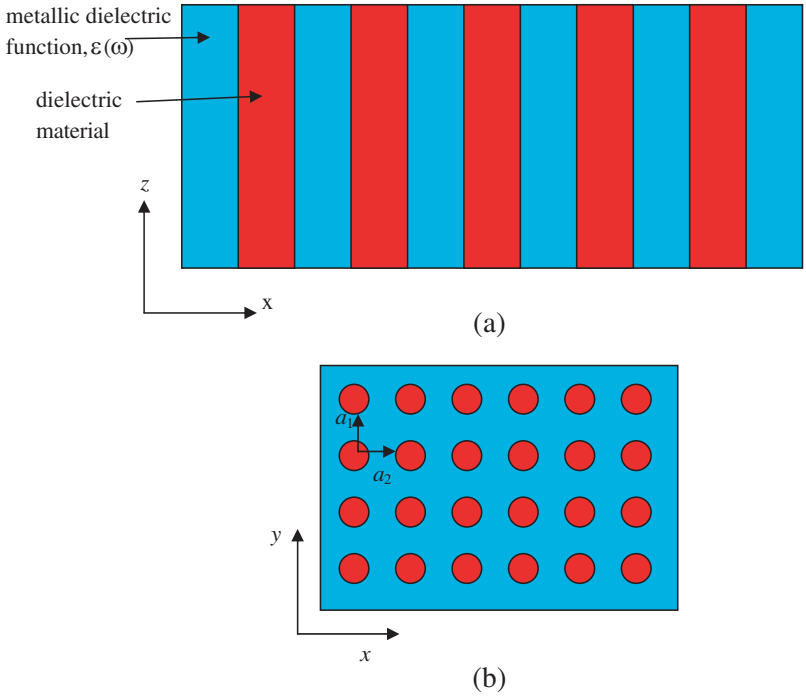

Figure 1. (a) Cross section view. (b) Top view of the 2D periodic structure.

So, we turned the Bravais lattice into vector form

$$x = l_1 a_1 + l_2 a_2 \tag{3}$$

The dielectric constant of the structure along x should fulfill the characteristics below

$$\varepsilon\left[x + x(l)\right] = \varepsilon\left(x\right) \tag{4}$$

Therefore, we expand it into Fourier form

$$\varepsilon'(x) = \sum_{G} \varepsilon'(G) e^{-iG \cdot x} \tag{5}$$

where G is the reciprocal lattice, and the Fourier coefficient is

$$\varepsilon'(G) = \frac{1}{a_c} \int_{G} d^2 x \varepsilon'(x) e^{-iG \cdot x} \tag{6}$$

where a_c is the lattice constant.

2.2. Modification

We modified and constructed the dielectric periodic function to meet the requirement of the metallic structure which we proposed and shown in Figure 1. We formulated it in (7).

$$\varepsilon(x) = \varepsilon(\omega) + [\varepsilon_o - \varepsilon(\omega)] \sum_{G'} S\left[x_{||} - x_{||}(l)\right] \tag{7}$$

where $S(x) = 1$ if x is inside the cross section of the cylinder centered at the origin of coordinates and $S(x) = 0$ if x outside this cross section.

Equation (7) is modified from the work of Kuzmiak [19]. The equation fulfills the periodic behavior of the structure.

$$\varepsilon(G) = \varepsilon(\omega)\delta_{0,G} + [\varepsilon_o - \varepsilon(\omega)]\frac{1}{a_c}\int d^2x_{||} S(x_{||}) e^{-iG_{||}\cdot x_{||}} \tag{8}$$

We transformed it in below equation

$$\varepsilon(G) = \begin{cases} \varepsilon(\omega) + f\left[\varepsilon_o - \varepsilon(\omega)\right], & G = 0 \\ f\left[\varepsilon_o - \varepsilon(\omega)\right] \dfrac{2J_1(G\cdot R)}{G\cdot R}, & G \neq 0 \end{cases} \tag{9}$$

where $f = \frac{1}{a_c}\int d^2x_{||} S(x_{||}) e^{-iG_{||}\cdot x_{||}}$ and $\frac{1}{a_c}\int\limits_G s(x) e^{-iG\cdot x} d^2x = 2f\frac{J_1(|G|R)}{|G|R}$.

2.3. Application

After the calculation of the dielectric function which is the most important part to find the band gap, we applied Maxwell's equation. In this application, we considered E polarization mode and H polarization mode.

In E polarization mode (TM):

$E_3(x|\omega)$ obtained in below

$$E_3(x|\omega) = \sum_G B(k|G) e^{i(k+G)\cdot x} \tag{10}$$

where k is the wave vector of the wave. Then, we obtained an Equation (11) satisfied by the coefficients $B(k|G)$

$$\begin{aligned} (k+G)^2 B(k|G) &= \frac{\omega^2}{c^2}\sum_{G'} \varepsilon\left(G - G'\right) B(k|G) \\ &= \frac{\omega^2}{c^2}\varepsilon(0) B(k|G) + \frac{\omega^2}{c^2}\sum_{G'} \varepsilon\left(G - G'\right) B(k|G) \end{aligned} \tag{11}$$

The results of Equation (9) is substituted into Equation (11) which transforms latter into

$$\mu^2 B(k|G) + \mu^2 \sum_{G'} (\varepsilon_o - 1) \frac{2fJ_1(|G-G'|R)}{|G-G'|R} B\left(k|G'\right) - \frac{\omega_p^2}{c^2} B(k|G)$$
$$- \sum_{G'} \frac{\omega_p^2}{c^2} \frac{2fJ_1(|G-G'|R)}{|G-G'|R} B\left(k|G'\right) - (k+G)^2 B\left(k|G\right) = 0 \qquad (12)$$

where $\mu = \frac{\omega}{c}$. Equation (12) is the final equation for the E polarization of metallic medium photonic crystals. This equation is used to plot the band structure of the photonic crystals. This equation has the form of a generalized eigenvalue problem. We employed the linearization technique to transform it into linear form. So, we rewrite Equation (12) in the form below

$$\mu^2 \overleftrightarrow{X} - \overleftrightarrow{Y} = 0 \qquad (13)$$

where the elements of the $NG \times NG$ matrices $\overleftrightarrow{A}$ and $\overleftrightarrow{B}$ are given by

$$\overleftrightarrow{X} = \sum_{G'} \partial_{0,G'} + f\left(\varepsilon_o - 1\right) \frac{2J_1|\left(G-G'\right)|R}{|\left(G-G'\right)|R} B\left(k|G'\right) \qquad (14)$$

$$\overleftrightarrow{Y} = \sum_{G'} \frac{\omega_p^2}{c^2} \partial_{0,G'} + (k+G)^2 \partial_{0,G'} + f\left[\frac{\omega_p^2}{c^2}\right] \frac{2J_1|\left(G-G'\right)|R}{|\left(G-G'\right)|R} B\left(k|G'\right) \qquad (15)$$

and NG is the number of plane waves used. Equation (13) represents the second order nonlinear problem, which can be represented in the equivalent matrix form $\overleftrightarrow{M}$

$$\overleftrightarrow{M} = \begin{pmatrix} 0 & \overleftrightarrow{X} \\ \overleftrightarrow{Y} & 0 \end{pmatrix} \qquad (16)$$

The complete solution of Equation (12) is obtained by solving for the eigenvalues of $\overleftrightarrow{M}$ by the diagonalization of this non-Hermitian matrix.

In H polarization mode (TE):

$H_3(x|\omega)$ obtained in below

$$H_3(x|\omega) = \sum_G A(k|G) e^{i(k+G)\cdot x} \qquad (17)$$

where k is the wave vector. Then, we obtained Equation (18) satisfied by the coefficients $A(k|G)$

$$\sum_{G'} (k+G) \cdot \left(k+G'\right) \hat{\kappa}(G-G') A(k|G') = \frac{\omega^2}{c^2} A(k|G) \qquad (18)$$

In H polarization, the periodic function is slightly different with the E polarization mode. We derived it in Equation (19)

$$\frac{1}{\varepsilon(x)} = \frac{1}{\varepsilon(\omega)} + \left[\frac{1}{\varepsilon_o} - \frac{1}{\varepsilon(\omega)}\right] \sum_l S\left[x - x(l)\right] \tag{19}$$

we transformed in the following equation

$$\hat{\kappa}(G) \begin{cases} \dfrac{1}{\varepsilon(\omega)} + \left[\dfrac{1}{\varepsilon_o} - \dfrac{1}{\varepsilon(\omega)}\right] f, & G = 0 \\ \left[\dfrac{1}{\varepsilon_o} - \dfrac{1}{\varepsilon(\omega)}\right] 2f \dfrac{J_1\left(|G|R\right)}{|G|R}, & G \neq 0 \end{cases} \tag{20}$$

where $f = \frac{1}{a_c}\int d^2x_{||} S(x_{||})$ and $\frac{1}{a_c}\int\limits_G s(x) e^{-iG\cdot x} d^2x = 2f\frac{J_1(|G|R)}{|G|R}$. Equation (20) is substituted into Equation (18) which transforms latter into:

$$\varepsilon_o \mu^2 A(k|G) - \mu \left[\begin{array}{l} \left(\varepsilon_o + \varepsilon_o \dfrac{c^2}{\omega_p^2} |k+G|^2\right) A(k|G) \\ + (1-\varepsilon_o) \dfrac{c^2}{\omega_p^2} \displaystyle\sum_{G'} (k+G)\cdot\left(k+G'\right) 2f \frac{J_1\left(|G-G'|R\right)}{|G-G'|R} A(k|G') \end{array} \right]$$

$$+ \frac{c^2}{\omega_p^2} \sum_{G'} (k+G)\cdot\left(k+G'\right) 2f \frac{J_1\left(|G-G'|R\right)}{|G-G'|R} A\left(k|G'\right) = 0 \tag{21}$$

Equation (21) is the final equation for the H polarization of metallic medium photonic crystals. This equation is used to plot the band structure of the photonic crystals. This equation has the form of a generalized eigenvalue problem. We employed the linearization technique to transform it into linear form. So, we rewrite Equation (21) in the form below

$$\mu^2 \overleftrightarrow{J} - \mu \overleftrightarrow{K} + \overleftrightarrow{L} = 0 \tag{22}$$

where the elements $NG \times NG$ matrices of $\hat{D}$, $\hat{E}$ and $\hat{F}$ are given by

$$\overleftrightarrow{K} = \left[\begin{array}{l} \left(\varepsilon_o + \varepsilon_o \dfrac{c^2}{\omega_p^2} |k+G|^2\right) A(k|G) \\ + (1-\varepsilon_o) \dfrac{c^2}{\omega_p^2} \displaystyle\sum_{G'} (k+G)\cdot(k+G') 2f \frac{J_1(|G-G'|R)}{|G-G'|R} A(k|G') \end{array} \right] \tag{23}$$

$$\overleftrightarrow{L} = \frac{c^2}{\omega_p^2} \sum_{G'} (k+G)\cdot\left(k+G'\right) 2f \frac{J_1\left(|G-G'|R\right)}{|G-G'|R} A\left(k|G'\right) \tag{24}$$

Equation (22) is the second order eigenvalue problems which can be represented as matrix below form

$$\overleftrightarrow{M} = \begin{pmatrix} 0 & I\overleftrightarrow{J} \\ \overleftrightarrow{K} & \overleftrightarrow{L} \end{pmatrix} \tag{25}$$

The complete solution of Equation (25) is obtained by solving for the eigenvalues of $\overleftrightarrow{M}$ by the diagonalization of this non-Hermitian matrix. So, the band structure of the E and H polarization modes can be plotted.

3. RESULTS AND DISCUSSION

We plotted the metallic-like photonic crystals in E polarization in which the filling fraction of the crystals is $f = 0.001$. This gives infinitesimally small spatial variation of the cylinder rods. We show the graph in Figure 2(a).

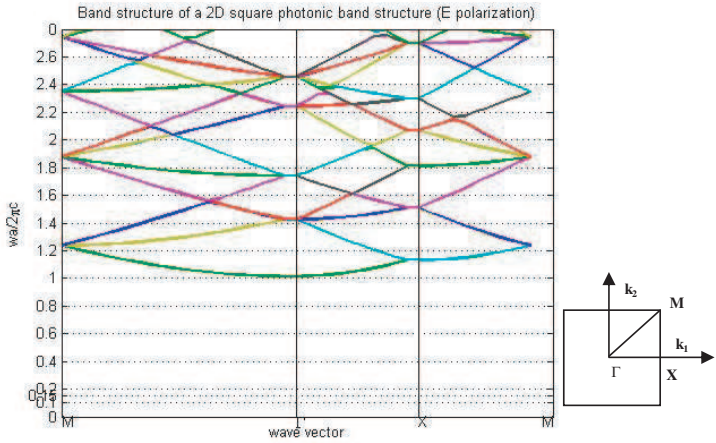

(a)

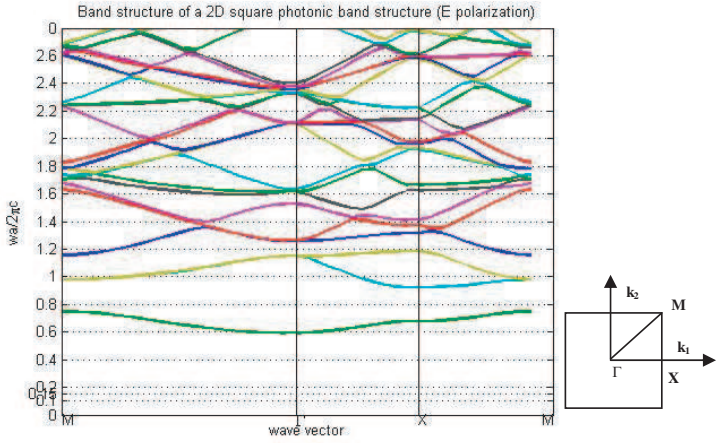

(b)

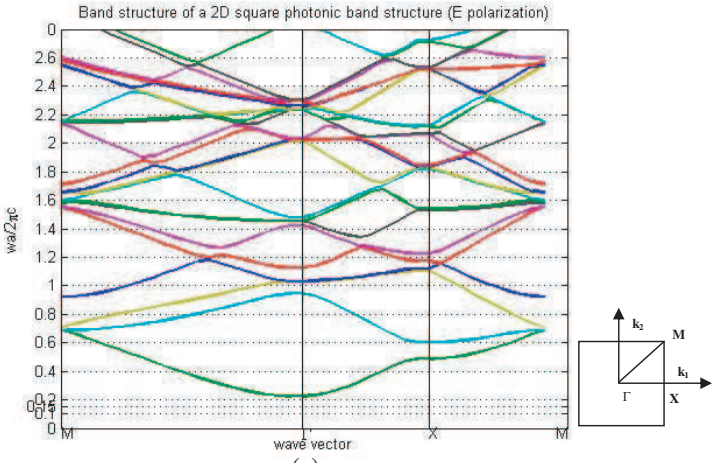

(c)

Figure 2. Band structure of E polarization mode for photonic crystals of vacuum rods in copper slab at (a) $f = 0.001$, (b) $f = 0.5$, (c) $f = 0.9$. (Square lattice).

We found that the graph is exhibited as a normal band energy graph of copper. It has a minimum frequency, $\frac{\omega a}{2\pi c} = 1$ at $k = 0$. This is the plasma frequency of copper. In bulk metal, this is the minimum frequency that wave can propagate. So, it is the same as effective plasma frequency. We found that when the metallic slab has dielectric material inside, the effective plasma frequency of the photonic crystals will change. So, we assumed that an array of vacuum rods was inserted inside the metallic slab with filling fraction $f = 0.5$. We have observed that the band graph is moved down as shown in Figure 2(b). From the graph, we found that there is a band gap in between two lowest energy bands which is from 0.7825 to 0.9077. The size of the gap is 0.1252. When we increased the radius of the vacuum, the gap size was reduced. At $f = 0.8$, the gap vanished. Figure 2(c) shows the graph of the band gap when filling fraction, $f = 0.9$. The two lowest bands are connected to each other. At the same time, the effective plasma frequency showed a decrease when filling fraction increased. We have theoretically depressed the effective plasma frequency into 400 THz range. We have thus reduced 80% of the copper's plasma frequency. The results are inspiring. But there is some limitation. One of the interesting characteristics of photonic crystals is the scaling law [20]. Under this law, dispersion curves are the same for the crystals which have similar dielectric functions. But, we found that scaling law is

not true when metallic material is used. This is due to the frequency-dependant dielectric constant of the metallic. Scaling law assumes that the dielectric function is independent of frequency. But when metallic is used, dielectric function of the photonic crystals changes with frequency. This makes the analysis of band energy of photonic crystals consist metallic or photonic crystals of metallic slab even harder. We have carried out the theoretical study of this structure.

The above discussion is for the band energy in E polarization mode. In the next section, the discussion is continued with H polarization. In this mode, the band energy graph is different from the E polarization mode.

We have plotted the band structure for H polarization when the filling fraction is extremely small which is $f = 0.001$ as shown in Figure 3(a). There are two parts in this graph. The lower part consists of straight lines, and the upper one is the ordinary energy band graph. So, there is a big gap in between these two parts. But, this gap is not suitable for the application in electronic devices. Straight lines in the graph are because wave is concentrated near the wall of vacuum rods. Although wave possesses energy, the wave is only near the surface and cannot propagate. This is the surface plasmon polaritons. The upper part of the band energy graph is the ordinary energy graph. It is the same as in the E polarization mode. It has a minimum frequency $\frac{\omega a}{2\pi c} = 1$ at $k = 0$. So, from the two results we found that the effective plasma frequency of two modes is the same if we neglect the surface plasmon effect in H polarization mode. In Figure 3(b), the graph represents the band energy of photonic crystals when filling

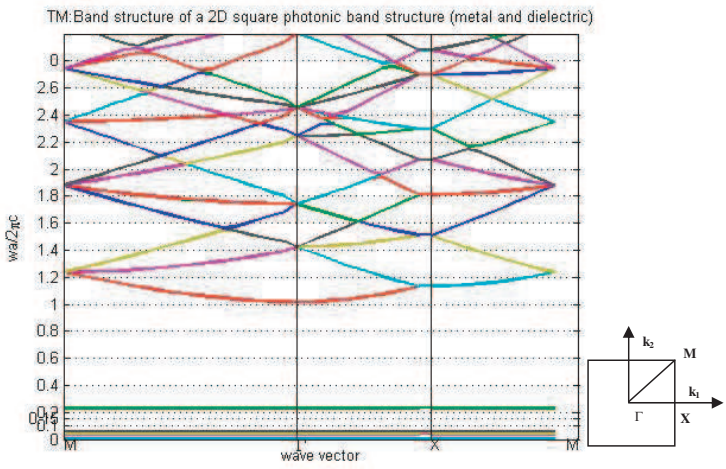

(a)

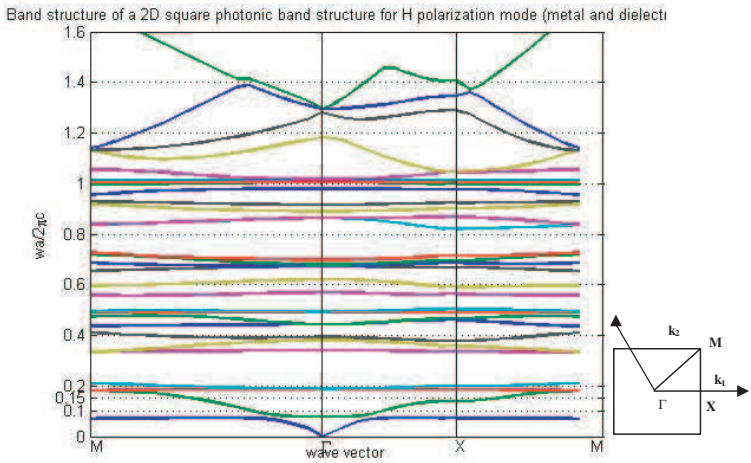

(b)

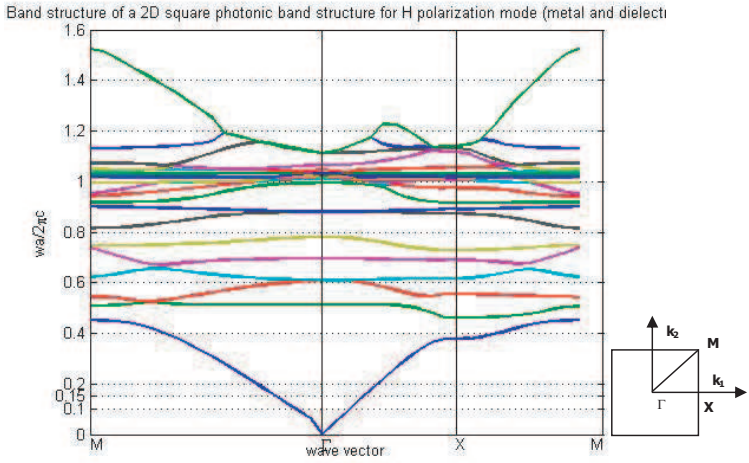

(c)

Figure 3. Band structure of H polarization mode for photonic crystals of vacuum rods in copper slab at (a) $f = 0.001$, (b) $f = 0.5$, (c) $f = 0.9$. (Square lattice).

fraction $f = 0.5$, and the effective plasma frequency is zero at $k = 0$. Figure 3(c) shows the band energy of photonic crystals when filling fraction $f = 0.9$. It also has zero effective plasma frequency at $k = 0$. But the difference between these two graphs is the first lowest band at M. Normalized frequency in Figure 3(b) is at 0.1 but in Figure 3(c) the normalized frequency is increased to 0.4. Then, Figure 3(b) has several band gaps in a certain range.

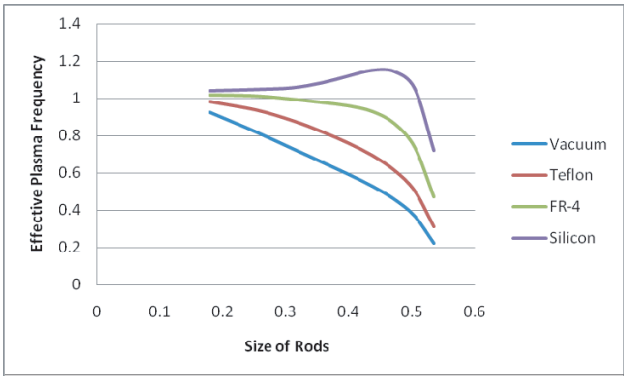

Figure 4. Effective plasma frequency versus size of dielectric rods for copper slab. (Square lattice).

We have done the calculation for metallic slab with different dielectric rods for E polarization mode (Equation (12)) and H polarization mode (Equation (21)). So, we investigate the changes of effective plasma frequencies when different sizes of materials are inserted into the metallic slab. We make a comparison in Figure 4. Vacuum ($\varepsilon_o = 1$), Teflon ($\varepsilon_o = 2$), FR-4 ($\varepsilon_o = 4.9$) and silicon ($\varepsilon_o = 13$) are used. The lattice constant used is 1 mm. So, the largest rods size is around 0.5 mm. From Figure 4, we observe that no matter which dielectric rods is used, the effective plasma frequency of photonic crystals with the extremely small rods in copper medium is 1. This is the plasma frequency of the copper. When the size of rods is increased, we find that the effective plasma frequency is decreased. As a result, the effective plasma frequency of metals can be depressed down when structure of copper is modified physically.

4. CONCLUSION

We successfully derived the general equation of photonic crystals containing dielectric rods in metals medium for H and E polarizations by using the plane wave expansion method. We have plotted the band energy graph of photonic crystals with dielectric rods in copper medium. We find that the effective plasma frequency of photonic crystals with different dielectric rods in copper medium is the same as the plasma frequency of copper when filing fraction is extremely small for E polarization mode. Then, we make a comparison of effective plasma frequency by vary the dielectric constant of rods. The effective plasma frequency is decreased when the filling fraction is increased. We

successfully depress more than 50% of the effective plasma frequency of copper by modifying it physically. So, we have shown that the effective plasma frequency of copper can be tailored with creating impurity in metals medium. It can be used in different applications which use metals medium. Our method of calculation can be extended to find the band gap structure of defect mode and waveguide mode of photonic crystals which is made of metals medium.

ACKNOWLEDGMENT

This project was carried out using the Fundamental Research Grants Scheme (FRGS) with grants number 203/PFIZIK/671166 and Posgraduate Research Grants Scheme (1001/PFIZIK/841028). We would like to thank the technical staff who participated in this project. Thanks are also extended to USM for their support and encouragement.

REFERENCES

1. Parui, S. K. and S. Das, "A simple electromagnetic bandgap structure for microstrip line," *Proceedings of the IEEE First India Annual Conference, INDICON*, 2004.
2. Chutinan, A., N. P. Kherani, and S. Zukotynski, "High-efficiency photonic crystal solar cell architecture," *Optics Express*, Vol. 17, 8, 2009.
3. Haase, C. and H. Stiebig, "Light trapping in thin-film silicon solar cells with periodic structures," *Conference Record of the 2006 IEEE 4th World Conference on Photovoltaic Energy Conversion*, Hawaii, 1509–1512, 2006.
4. Guenneu, S., A. Nicolet, F. Zolla, and S. Lasquellec, "Numerical and theoretical study of photonic crystal fibers," *Progress In Electromagnetics Research*, PIER 41, 271–305, 2003.
5. Nozhat, N. and N. Granpayeh, "Specialty fibers designed by photonic crystals," *Progress In Electromagnetics Research*, PIER 99, 225–244, 2009.
6. Ozbay, E., B. Temelkuran, and M. Bayindir, "Microwave applications of photonic crystals," *Progress In Electromagnetics Research*, PIER 41, 185–209, 2003.
7. Kuzmiak, V. and A. A. Maradudin, "Distribution of electromagnetic field and group velocities in two-dimensional periodic systems with dissipative metallic components," *Physical Review B*, Vol. 58, 22, 1998.

8. Pendry, J. B., "Extremely low frequency plasmons in metallic mesostructures," *Physical Review Letters*, Vol. 76, 4, 1996.
9. Brand, S., R. A. Abram, and M. A. Kaliteevski, "Complex photonic band structure and effective plasma frequency of a two-dimensional array of metal rods," *Physical Review B*, Vol. 75, 7, 2007.
10. Hermann, D., M. Frank, K. Busch, and P. Wolfle, "Photonic band structure computations," *Optics Express*, Vol. 8, Jan. 29, 2001.
11. Plihal, M. and A. A. Maradudin, "Photonic band structure of two-dimensional systems: The triangular lattice," *Physical Review B*, Vol. 44, 7, 1991.
12. Kuzmiak, V., A. A. Maradudin, and F. Pincemin, "Photonic band structures of two-dimensional systems containing metallic components," *Physical Review B*, Vol. 50, 10, 1994.
13. Zhou, Y.-S., B.-Y. Gu, and F.-H. Wang, "Photonic band gap structures and guide modes in two-dimensional magnetic photonic crystal heterostructures," *European Physics Journal B*, Vol. 37, 7, 2004.
14. Guo, S. and S. Albin, "Simple plane wave implementation for photonic crystal calculations," *Optics Express*, Vol. 11, 9, Jan. 27, 2003.
15. Rambabu, K., M. Mokhtaari, and J. Borneman, "Simplified computation of electromagnetic band-gap properties of via-holed metal patches," *IEEE International Symposium on Electromagnetic Compatibility, EMC*, 2007.
16. Qi, L.-M. and Z. Yang, "Modified plane wave method analysis of dielectric plasma photonic crystal," *Progress In Electromagnetics Research*, PIER 91, 319–332, 2009.
17. Low, K. L., M. Z. M. Jafri, and S. A. Khan, "Band gap study using plane wave expansion method for metallic slab with air rods in E polarizing mode," *Chinese Journal of Physics*, Vol. 47, 10, 2009.
18. Xu, X., Y. Xi, D. Han, X. Liu, J. Zi, and Z. Zhu, "Effective plasma frequency in one-dimensional metallic-dieletric photonic crystals," *Applied Physics Letters*, Vol. 86, 3, 2005.
19. Kuzmiak, V. and A. A. Maradudin, "Photonic band structures of one- and two-dimensional periodic systems with metallic components in the presence of dissipation," *Physical Review B*, Vol. 55, 18, 1997.
20. Sakoda, K., *Optical Properties of Photonic Crystals*, 2005.